Human milk oligosaccharides and non-digestible carbohydrates reduce pathogen adhesion to intestinal epithelial cells by decoy effects or by attenuating bacterial virulence

Kong, Chunli; de Jong, Anne; de Haan, Bart J; Kok, Jan; de Vos, Paul

Published in:
Food Research International

DOI:
10.1016/j.foodres.2021.110867

Food Research International 151 (2022) 110867

Contents lists available at ScienceDirect

Food Research International

journal homepage: www.elsevier.com/locate/foodres

Human milk oligosaccharides and non-digestible carbohydrates reduce pathogen adhesion to intestinal epithelial cells by decoy effects or by attenuating bacterial virulence

Chunli Kong [a,b,*], Anne de Jong [c], Bart J. de Haan [b], Jan Kok [c], Paul de Vos [b]

[a] School of Food and Health, Beijing Engineering and Technology Research Center of Food Additives, Beijing Advanced Innovation Center for Food Nutrition and Human Health, Beijing Technology and Business University, 100048 Beijing, China
[b] Immunoendocrinology, Division of Medical Biology, Department of Pathology and Medical Biology, University of Groningen and University Medical Center Groningen, Hanzeplein 1, 9700 RB Groningen, the Netherlands
[c] Groningen Biomolecular Sciences and Biotechnology Institute, Department of Molecular Genetics, University of Groningen, Nijenborgh 7, 9747 AG Groningen, the Netherlands

ARTICLE INFO

Keywords:
Fucosyllactose
Pectin
Inulin
Infection
Virulence
Transcriptomics analysis

ABSTRACT

This work investigated the effects of different chemical structures of human milk oligosaccharides (hMOs) and non-digestible carbohydrates (NDCs) on pathogen adhesion by serving as decoy receptors. Pre-exposure of pathogens to inulins and low degree of methylation (DM) pectin prevented binding to gut epithelial Caco2-cells, but effects were dependent on the molecules' chemistry, pathogen strain and growth phase. Pre-exposure to 3-fucosyllactose increased *E. coli* WA321 adhesion (28%, $p < 0.05$), and DM69 pectin increased *E. coli* ET8 (15 fold, $p < 0.05$) and *E. coli* WA321 (50%, $p < 0.05$) adhesion. Transcriptomics analysis revealed that DM69 pectin upregulated flagella and cell membrane associated genes. However, the top 10 downregulated genes were associated with lowering of bacteria virulence. DM69 pectin increased pathogen adhesion but bacterial virulence was attenuated illustrating different mechanisms may lower pathogen adhesion. Our study illustrates that both hMOs and NDCs can reduce adhesion or attenuate virulence of pathogens but that these effects are chemistry dependent.

1. Introduction

Breastfeeding is the gold standard for healthy development of newborns. Mother milk consists of substantial amounts of bioactive molecules which not only provide nutrients but also support gut microbiota development and gut immune barrier maturation (Cheng, Akkerman, Kong, Walvoort, & de Vos, 2020). However, due to various reasons, there are still about 70% of infants that cannot be solely fed with mother milk, and need to consume cow milk-derived infant formula (Heymann, Raub, & Earle, 2013). Compared to mother milk, cow milk lacks a unique family of molecules (Urashima, Taufik, Fukuda, & Asakuma, 2013), *i.e.* human milk oligosaccharides (hMOs), which have been demonstrated to have many beneficial functions for infants such as stimulation of colonization of gut commensals (Asakuma et al., 2011), inhibition of infection by gut pathogens (Ruiz-Palacios, Cervantes, Ramos, Chavez-Munguia, & Newburg, 2003), and enhancing gut immune barrier function (Holscher, Bode, & Tappenden, 2017). Non-digestible carbohydrates (NDCs) such as inulins and pectins are added to infant formula to mimic some functions of hMOs. During recent years also synthetic hMOs are produced in a cost-effective way and added as supplements to infant formula (Cheng et al., 2020).

One important function of hMOs and NDCs in infant formula is to reduce gut pathogen infection (Chen, Reiter, Huang, Kong, & Weimer, 2017). Adherence to the gut epithelium is often the first step for pathogens to initiate an infection (Berne, Ellison, Ducret, & Brun, 2018). HMOs have been postulated to have similar chemical structures as present on the gut epithelial glycocalyx (Bode & Jantscher-Krenn, 2012), allowing the hMOs to serve as decoy for gut pathogens in the

Abbreviations: **DEGs**, differentially expressed genes; **DM**, degree of methylation; **DP**, degree of polymerization; **FL**, fucosyllactose; **GO**, gene ontology; **hMO**, human milk oligosaccharide; **MDS**, Multi-dimensional scaling; **NDC**, non-digestible carbohydrate.

* Corresponding author at: School of Food and Health, Beijing Engineering and Technology Research Center of Food Additives, Beijing Advanced Innovation Center for Food Nutrition and Human Health, Beijing Technology and Business University, 100048 Beijing, China.
E-mail address: c.kong@umcg.nl (C. Kong).

https://doi.org/10.1016/j.foodres.2021.110867
Received 24 August 2021; Received in revised form 14 November 2021; Accepted 2 December 2021
Available online 7 December 2021

lumen of the intestine and blocking the ability of pathogens to adhere to gut epithelium (Thöle, Brandt, Ahmed, & Hensel, 2015). However this probably applies to specific hMO structures as anti-adhesive effects of hMOs on gut pathogens were different for 3-fucosyllactose (3-FL), 2′-fucosyllactose (2′-FL), 3′-sialyllactose (SL), and 6′-SL as only 3-FL inhibited the adhesion of enterotoxigenic *Escherichia coli* (ETEC) and *Salmonella fyris* (Coppa et al., 2006) to Caco-2 cells. The structure-dependent effect on the adhesion of pathogens was not exclusive to hMOs but also observed for NDCs such as okra pectin extracts, in which pectins with saturation levels of 60% and 90% but not the 30% fractions inhibited *Helicobacter pylori* adhesion to human gastric cells (Thöle et al., 2015).

Flagella, pili, and outer membrane proteins are important structures for pathogens to move and adhere to gut epithelial cells (Berne et al., 2018). These structures are mainly composed of extracellular proteins, and play an important role in anchoring to epithelial cells (Berne et al., 2018). However, these proteins are differently expressed in pathogens in different growth phases (Jaishankar & Srivastava, 2017). Compared to the logarithmic (log) phase of growth, the cell of gram negative bacteria in stationary phase turns to spherical, with increased thickness of peptidoglycan of the outer membrane, increased resistance to environment stress, and biofilm formation (Jaishankar & Srivastava, 2017). All these changes might influence the bacteria-host interaction. For example, *Escherichia (E.) coli* K12 cells in stationary phase are notably more adhesive than those in the log phase (Walker, Hill, Redman, & Elimelech, 2005). In contrast, both enteropathogenic and enterohemorrhagic *E. coli* express virulence genes during the log growth phase which include the type 3 secretion system mediating intimate pathogen binding to the plasma membrane of host epithelia (Daniell et al., 2001). Besides adhering to epithelial cells, other virulence factors including endotoxin also contribute to bacterial pathogenesis. An example is enterobactin, which can be used to capture iron from the host, and is produced by *Escherichia* and *Salmonella* species (Peterson, 1996).

Understanding how individual hMOs or NDCs interact with pathogens is important for the design of "tailored" infant formula for infants with different health requirements, such as for children at risk for pathogenic infections (Carvalho et al., 2020; Ihekweazu & Versalovic, 2018). Although some studies have demonstrated that hMOs and NDCs can inhibit gut pathogen adhesion, the effects of individual molecules or its chemistry are still largely unknown. Here a hypothesis was raised that these molecules could inhibit adhesion of specific pathogens and influence pathogen behavior through a so-called decoy effect. To this end, the pathogens were pre-incubated with different hMOs and NDCs before exposing them to intestinal epithelial cells to model the luminal decoy effects of these molecule. These molecules include hMOs of 2'-FL, which has been already included in infant formula, and 3-FL, and NDCs which are often used as substitutes in infant formula, *i.e.* inulins with different degrees of polymerization (DP) (DP3-DP10, DP10-DP60, DP30-60) and pectins with different degrees of methylation (DM) (DM7, DM55, DM69). Effects were tested on the adhesion of gut diarrhea pathogens including *E. coli* ET8, *E. coli* LMG5862, *E. coli* O119, *E. coli* WA321, *Salmonella enterica* subsp *enterica* LMG07233, and one lung pathogen *Klebsiella pneumoniae* LMG20218 to determine enteric pathogen specificity of the effects. As some NDCs and hMOs enhanced the adhesion of certain gut pathogens, for the first time, these combinations were examined by investigating the bacterial transcriptomes to determine which genes are up-regulated and have to be held responsible for possible enhanced adhesion or bacterial virulence.

2. Material and methods

2.1. Carbohydrates

The short chain human milk oligosaccharides (hMOs), 2′-FL and 3-FL were provided by Elicityl (Grenoble, France). Chicory inulins with different degree of polymerization (DP3-DP10, DP10-DP60, and DP30-DP60) were provided by Sensus (Eindhoven, the Netherlands). DP3-DP10 is the highly soluble powdered Frutafit® CLR inulin, DP10-DP60 and DP30-DP60 are the moderate soluble powdered Frutafit® TEX! inulins. Commercially extracted lemon pectins with different degree of methylation (DM7, DM55, and DM69) were obtained from CP Kelco (Copenhagen, Denmark).

2.2. Enteric pathogens and culture

The pathogen strain *Escherichia (E.) coli* O119 was purchased from ATCC. The strains *E. coli* ET8, *E. coli* LMG5862, *E. coli* WA321, *Salmonella (S.) enterica* subsp *enterica* LMG07233, and the lung pathogen *Klebsiella (K.) pneumoniae* LMG20218 were kindly provided by Prof. Oscar Kuipers, Department of Molecular Genetics, University of Groningen (Groningen, the Netherlands). The lung pathogen *K. pneumoniae* LMG20218 was chosen to determine specificity of effects for gut microbiota. *E. coli* ET8 and *E. coli* WA321 are soil isolates. *E. coli* LMG5862, *S. enterica* subsp *enterica* LMG07233, and *K. pneumoniae* LMG20218 are available from the Belgian Coordinated Collections of Microorganisms (BCCM). The serotypes of the strains *E. coli* O119 and *E. coli* WA321 are *E. coli* O119: K69 and *E. coli* WA321 O16: H48. The serotypes for other strains are unknown. Bacterial strains were grown on brain heart infusion (BHI) agar plates. Single colonies were cultured overnight in BHI broth in a shaking incubator (220 rpm) under aerobic conditions at 37 °C, and sub-cultured until either log phase or stationary phase was reached. The cultures were harvested by centrifugation and resuspended in Phosphate buffered saline (PBS). Before use, the optical density (OD) at 600 nm was adjusted to 0.6 ± 0.02 (approx. 1×10^9 CFU/ml), after which the cells were washed once in PBS, and concentrated in 50% volume of antibiotic-free cell culture medium before inoculation.

2.3. Cell line

Human colon carcinoma Caco-2 cells (HTB-37, 2012, ATCC) at passage 15–20 were routinely cultured at 5% CO_2 at 37 °C in Dulbecco's Modified Eagle Medium (DMEM, Lonza, Verviers, Belgium), supplemented with 10% (v/v) fetal bovine serum (FBS, Invitrogen, Breda, the Netherlands), 1% (v/v) non-essential amino acid, 50 U/ml Penicillin, 50 μg/ml Streptomycin, and 2.5% (v/v) 4-(2-hydroxyethyl)-1-piperazineethanesulfonic acid (HEPES, Sigma, Zwijndrecht, the Netherlands). The cell density was adjusted to 3×10^4/ml before seeding onto 24-well plates and the cells were cultured for 21 d.

2.4. Dosage information

All of the carbohydrates were dissolved to 2 mg/ml in antibiotic-free cell culture medium. The concentration was optimized in a pilot study where 2 mg/ml, 5 mg/ml, and 10 mg/ml were compared. We decided to use 2 mg/ml as this concentration elicited a sufficient strong response and also it is within the range of susceptibility of the cells we have used as shown in other studies (Kiewiet et al., 2018; Kong et al., 2019). The bacterial growth after incubation with the carbohydrate molecules was also studied with BioTeck (data not shown), and no toxicity on the bacteria was observed.

2.5. Infection and anti-adhesion assay

In order to explore the anti-adhesion effects of the dietary molecules on the pathogens, the pathogenic bacteria were pre-incubated with carbohydrate molecules to identify a possible decoy effect. As expression of bacterial-host molecules differ between log and stationary phase (Walker et al., 2005), the pathogens taken from both growth phases were tested.

Pathogens were pre-incubated with the carbohydrates in cell culture

medium for 2 h and then transferred to Caco-2 cells and further incubated at 37 °C in 5% CO_2 incubator for 1 h (*E. coli* LMG5862) or 2 h (all the other strains). Incubation time with *E. coli* LMG5862 was shorter as it interfered with integrity of Caco-2 cells. The integrity of Caco-2 cells monolayer was determined with light microscope directly after the infection. Pathogens incubated with medium without carbohydrates served as controls. After the infection, the non-adherent bacteria were gently washed away with PBS for three times. The adherent bacteria were quantified by incubating Caco-2 cells with 200 μl of 0.1% Triton-X100 for 10–15 min. A volume of 100 μl of the released bacteria was subjected to serial dilutions. The dilution factor was determined according to the CFU countable range using the drop-plate method, which is 3–30 colonies on BHI agar plates per 10 μl (Herigstad, Hamilton, & Heersink, 2001). A volume of 60 μl of the bacteria dilutions of each treatment for one experiment was plated and the BHI agar plates were cultured overnight at 37 °C in 5% CO_2 incubator. Results were expressed as relative adhesion compared to controls.

2.6. Total RNA isolation and RNA sequencing

Outcome of the pathogen adhesion studies led to selection of strains for RNA-seq studies. To this end, *E. coli* ET8 in log phase incubated with or without DM69 pectin, *E. coli* WA321 in log phase incubated with or without 3-FL, and *E. coli* WA321 in stationary phase incubated with or without DM69 pectin were collected by centrifugation, snap frozen in liquid nitrogen, and stored at −80 °C (n = 3). Total RNA was isolated using a high pure RNA isolation kit (Roche Diagnostics, Almere, the Netherlands). The bacterial cell pellets were thawed on ice, resuspended in 400 μl of ice cold TE (10 mM Tris-HCl, 1 mM EDTA) buffer in diethyl pyrocarbonate (DEPC) and added to screw-cap tubes containing 500 mg glass-beads (75–150 μm), 50 μl of 10% sodium dodecyl sulfate (SDS), and 500 μl of acid-phenol:chloroform (pH 4.5, with indoleacetic acid, 125:24:1). The bacteria were disrupted by 2 times fast shaking for 45 s in a Biospec Mini-BeadBeater (Biospec Products, Bartlesville, OK, USA) with an intermediate cooling step on ice for 1 min. The suspension was centrifuged at 10,000*g* for 10 min. Subsequently, 500 μl of the upper phase containing nucleic acids was transferred to a new tube with 400 μl of chloroform, mixed by vortexing and centrifuged at 10,000*g* for 5 min. The upper phase was transferred to a new tube and 1 ml of Lysis/Binding buffer was added and mixed by inverting several times. The homogeneous mixture was passed through a filter tube by centrifugation at 8,600*g* for 15 s after which the nucleic acids remained on the filter. DNA was removed by adding 100 μl of DNase l mix (10 μl DNase I in 90 μl DNase buffer) and incubating at room temperature for 1 h. Afterwards, the RNA pellet on the filter was washed by adding 500 μl wash buffer I and centrifuged at 8,600*g* for 15 s, then washed by adding 500 μl wash buffer II and centrifuged at 8,600*g* for 15 s, and finally washed by adding 200 μl wash buffer II and centrifuged at 10,000*g* for 2 min. The RNA on the filter was dissolved in 50 μl elution buffer and incubated for 10 min at room temperature and collected in a new tube by centrifugation at 8,600*g* for 1 min and stored at −80 °C. RNA concentration was measured using a NanoDrop ND-1000 (Thermo Fisher Scientific). RNA quality was confirmed with an Agilent 2100 Bioanalyzer (Agilent Technologies, Waldbronn, Germany) by measuring the integrity of rRNA (23S/16S > 1.6) and determining any contamination (260/230 > 1.7, and 260/280 > 1.7). RNA-seq was performed by BGI Genomics Corporation (Hongkong).

2.7. RNA-seq data analysis

Raw sequencing reads were first tested for quality and trimmed with a PHRED score over 28. Read alignment of *E. coli* ET8 was performed based on the genome sequence of *E. coli* K12; that of *E. coli* WA321 was performed based on the genome sequence of *E. coli* WA321. The aligned reads per kilobase per million reads (RPKM), the experimental factors, and the contrasts for the comparisons were used as the input for the T-REx analysis pipeline (de Jong, van der Meulen, Kuipers, & Kok, 2015). T-REx was used for all the statistical analysis of the RNA-seq data based on EdgeR. The functional analysis of RNA-seq data was performed in GSEA-Pro (http://gseapro.molgenrug.nl/) and the functions were classified with gene ontology (GO).

2.8. Statistical analyses

The anti-adhesion effect test data were analyzed by GraphPad Prism 6 software (GraphPad Prism Software Inc. San Diego, USA). The pathogen adhesion data were normalized to control by setting control as 1. The Kolmogorov-Smirnov test was done to determine the normality of data distribution. Results were expressed as mean ± SD. All data were finally analyzed with Kruskal-Wallis test One-way ANOVA with Dunn's multiple comparisons test. Significant difference was defined as $p < 0.05$ (*$p < 0.05$, **$p < 0.01$).

3. Results

3.1. Decoy effects induced by hMOs

Log phase. Pre-incubation of log phase bacterial cultures with hMOs did not significantly inhibit adherence (Fig. 1). Although adhesion of *E. coli* O119 was reduced when pre-incubated with 2′-FL this was not statistically significant. However, adherence of *E. coli* WA321 was significantly increased and not decreased when pre-incubated with 3-FL ($p < 0.05$, Fig. 1D). Adherence of the other pathogens was unchanged by pre-incubation with 3-FL.

Stationary phase. Pre-incubating the pathogens in stationary phase with 2′-FL and 3-FL did not influence their adhesion to Caco-2 cells (Fig. 1G-L).

3.2. Decoy effects induced by inulins

Log phase. Pre-incubating pathogens taken from the log phase with inulins reduced the adhesion of most of the pathogens in a DP-dependent manner (Fig. 2A-F). DP3-DP10 significantly reduced the adhesion of *E. coli* O119 with 70% ($p < 0.05$, Fig. 2C). DP30-DP60 inulin reduced adhesion of *E. coli* LMG5862, *E. coli* WA321, and *K. pneumoniae* LMG20218, with 14% ($p < 0.05$, Fig. 2B), 11% ($p < 0.05$, Fig. 2D), and 29% ($p < 0.01$, Fig. 2F), respectively.

Stationary phase. Pre-incubation of pathogens in the stationary phase with inulins did not significantly reduce adhesion of the pathogens to Caco-2 cells (Fig. 2G-L). Adhesion of *E. coli* ET8 (Fig. 2G) and *K. pneumoniae* LMG20218 (Fig. 2L) was reduced by DP30-DP60, with a reduction of 21% and 42% respectively, but no significant difference was observed. Other pathogens were not affected by pre-incubation with inulins.

3.3. Decoy effects induced by pectins

Log phase. Pectins had anti-adhesion effects on pathogens taken from log phase in a DM-dependent way. Unexpectedly, pre-incubating with DM69 pectin increased the adhesion of *E. coli* ET8 to Caco-2 cells ($p < 0.05$, Fig. 3A) as much as 15 fold. DM69 pectin also significantly increased the adhesion of *S. enterica* subsp *enterica* LMG07233 to Caco-2 cells by 50% ($p < 0.05$, Fig. 3E). However, DM55 pectin significantly inhibited the adhesion of *K. pneumoniae* LMG20218 to Caco-2 cells (27%, $p < 0.05$, Fig. 3F).

Stationary phase. Pre-incubating the pathogens taken from stationary phase with pectins resulted in even more pronounced effects. DM7 pectin significantly reduced the adhesion of *E coli* O119 to Caco-2 by 31% ($p < 0.05$, Fig. 3I). DM55 pectin reduced adhesion of *E. coli* LMG5862 by 36.73% ($p < 0.01$, Fig. 3H) and of *K. pneumoniae* LMG20218 by 28.30% (Fig. 3L). However, DM69 pectin had both increasing and diminishing effects depending on the pathogen tested. It

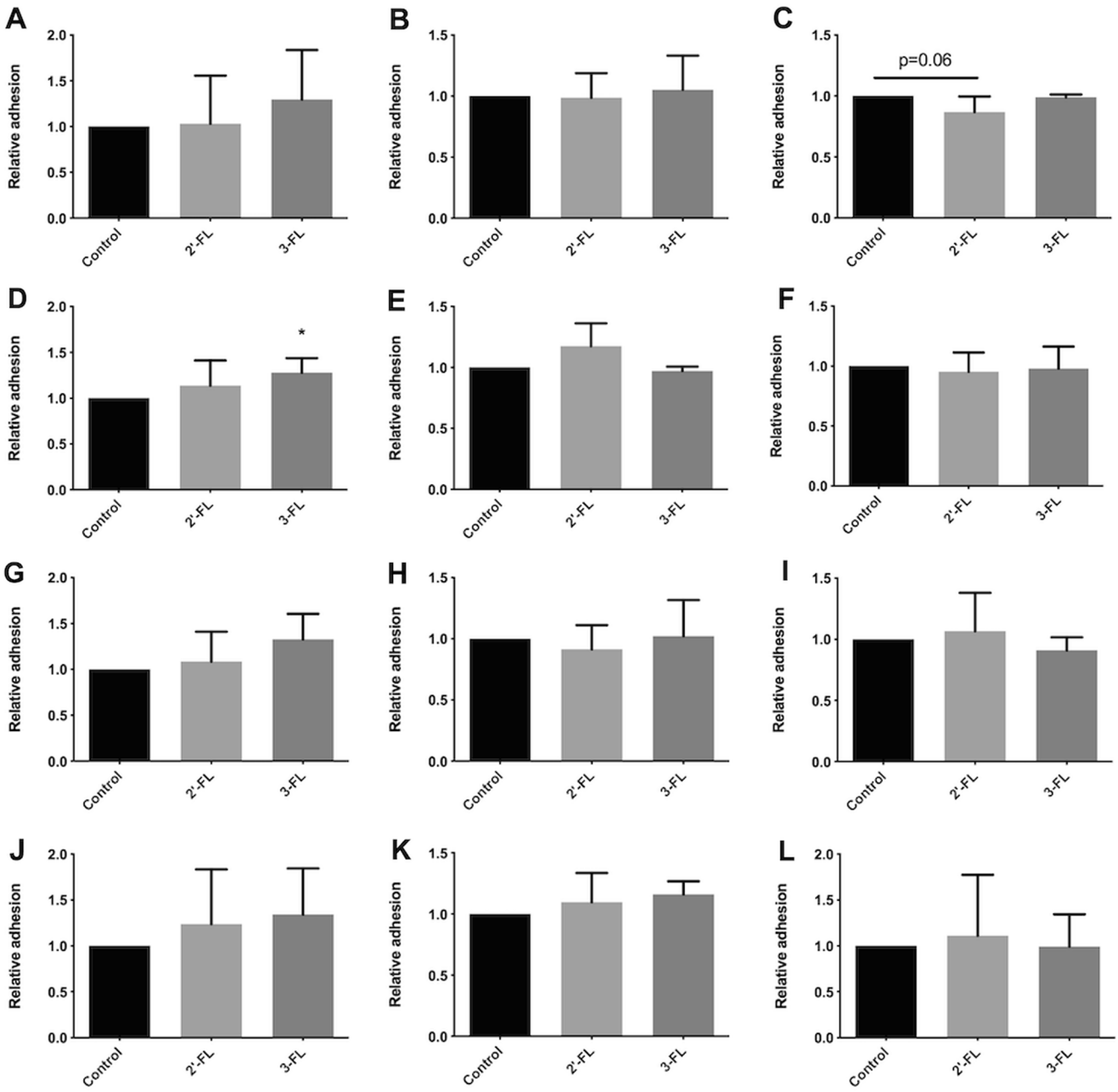

Fig. 1. Decoy effects of hMOs on the relative adhesion of pathogens harvested from log and stationary growth phase to gut epithelial Caco-2 cells. Caco-2 cells were cultured for 21 d until confluency. Pathogens were harvested from log or stationary growth phase. The hMOs 2′-FL and 3-FL were pre-incubated with the pathogens from log phase, *i.e. E. coli* ET8 (A), *E. coli* LMG5862 (B), *E. coli* O119 (C), *E. coli* WA321 (D), *S.* LMG07233 (E), and *K. pneumoniae* LMG20218 (F) or in stationary phase *i.e. E. coli* ET8 (G), *E. coli* LMG5862 (H), *E. coli* O119 (I), *E. coli* WA321 (J), *S.* LMG07233 (K), and *K. pneumoniae* LMG20218 (L) for 2 h. After pre-incubated the individual pathogen with either 2′-FL or 3-FL, the pathogen was applied to Caco-2 cells for another 2 h. After infection, the total colony forming units (CFUs) of pathogens adhered to Caco-2 cells were determined by a drop-plating method. The group without hMO served as control. All data was expressed as mean ± SD from five experiments. Statistical significance was tested with one-way ANOVA (*$p < 0.05$).

significantly reduced the adhesion of *E. coli* LMG5862 (28%, $p < 0.05$, Fig. 3H), while significantly increased the adhesion of *E. coli* WA321 (50%, $p < 0.05$, Fig. 3J).

3.4. Differentially expressed genes (DEGs) in response to DM69 pectin and 3-FL

To explore possible mechanisms by which DM69 pectin and 3-FL can increase instead of reducing adhesion to gut epithelial cells, transcriptomics analyses were performed. As DM69 pectin strongly enhanced adhesion of *E. coli* ET8 from log phase, and *E. coli* WA321 from stationary phase, and 3-FL increased adhesion of *E. coli* WA321 from log phase to Caco-2 cells, these strains were selected. Multi-dimensional scaling (MDS) plots (Figure S1A and S1B) were made with output data from edgeR. The distance between different experimental groups is larger than that between the biological replicates within an experimental group, indicating there was more variability between than within experimental groups. Subsequently, analyses were performed on the differentially expressed genes.

3.4.1. E. coli ET8

Pre-incubation with DM69 pectin of *E. coli* ET8 from log phase led to

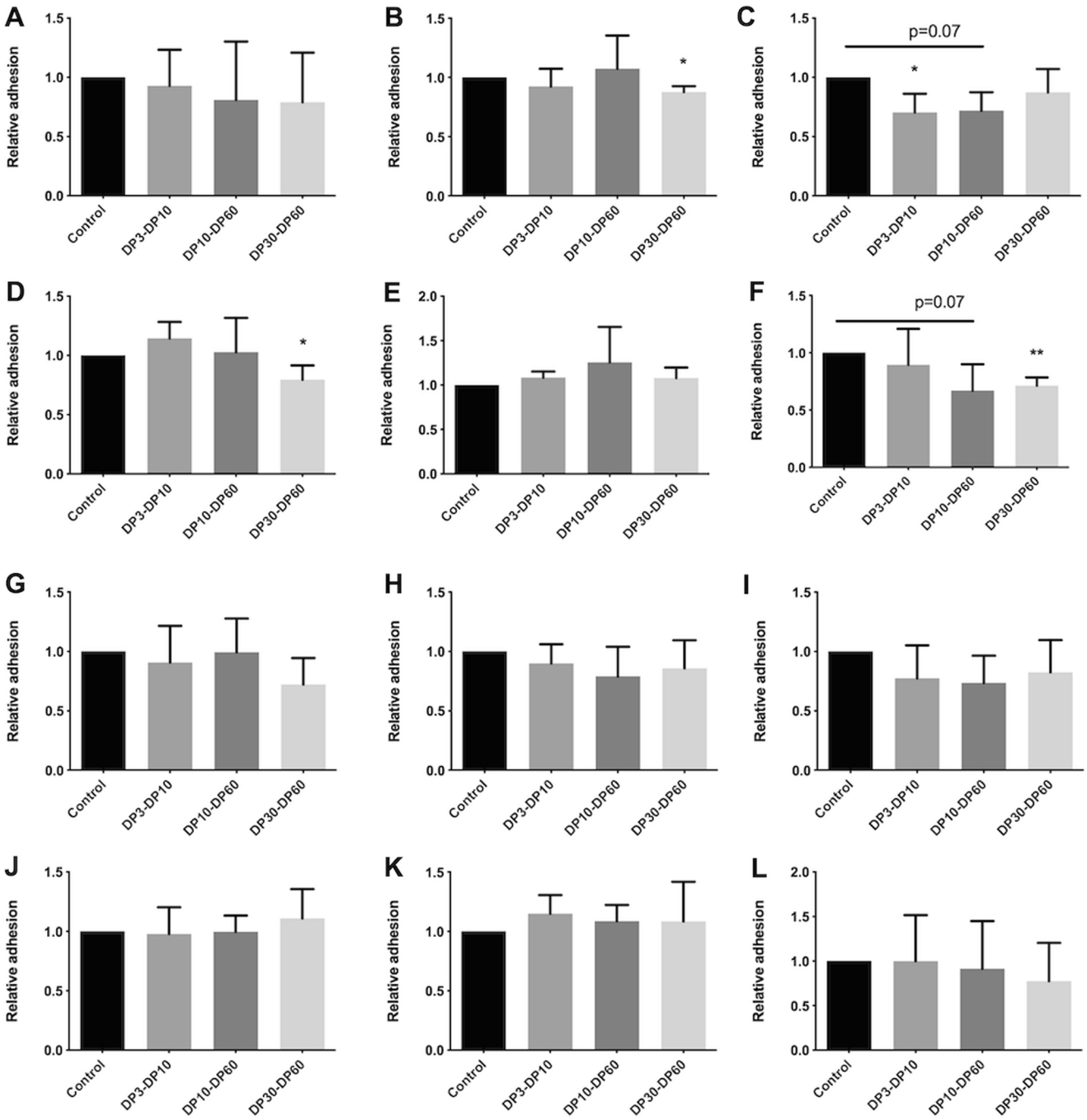

Fig. 2. Decoy effects of inulins on the relative adhesion of pathogens harvested from log and stationary growth phase to gut epithelial Caco-2 cells. Caco-2 cells were cultured for 21 d until confluency. Pathogens were harvested from log or stationary growth phase. The inulins DP3-DP10, DP10-DP60, and DP30-DP60 were pre-incubated with the pathogens from log phase, *i.e. E. coli* ET8 (A), *E. coli* LMG5862 (B), *E. coli* O119 (C), *E. coli* WA321 (D), *S.* LMG07233 (E), and *K. pneumoniae* LMG20218 (F) or in stationary phase *i.e. E. coli* ET8 (G), *E. coli* LMG5862 (H), *E. coli* O119 (I), *E. coli* WA321 (J), *S.* LMG07233 (K), and *K. pneumoniae* LMG20218 (L) for 2 h. After pre-incubated the individual pathogen with either DP3-DP10, DP10-DP60, or DP30-DP60, the pathogen was applied to Caco-2 cells for the infection for another 2 h. After infection, the total colony forming units (CFUs) of pathogens adhered to Caco-2 cells were determined by a drop-plating method. The group without inulin served as control. All data was expressed as mean ± SD from five experiments. Statistical significance was tested with one-way ANOVA (**$p < 0.01$, *$p < 0.05$).

over 350 genes being up regulated and more than 180 genes being down regulated. Heatmap analysis (Figure S2) shows the mean value (log2 based) of the group with and without DM69 pectin stimulation. The volcano plot (Fig. 4B) shows the distribution of all genes that are differentially expressed upon treatment of the cells with DM69 pectin.

As shown in Fig. 4C and Table S1, upon pre-incubation with DM69 pectin, the top 10 significantly up regulated genes of *E. coli* ET8 from log phase were *gatZ*, *hyaA*, *hycB*, *ydjX*, *hycA*, *hycD*, *hyaF*, *mcrB*, *ymfG*, and *hycF*. The most significantly up regulated gene, *gatZ*, is annotated as encoding the D-tagatose-1,6-bisphosphate aldolase subunit (GatZ). The top 10 significantly down regulated genes (Fig. 4C and Table S1) were *nrdF*, *fepA*, entB, entE, entC, nrdI, *nrdH*, *yncE*, *cirA*, and *nrdE*.

3.4.2. *E. coli* WA321

E. coli WA321 showed enhanced adhesion with both 3-FL (Fig. 1D) and DM69 pectin (Fig. 3J) and was therefore further studied. Gene

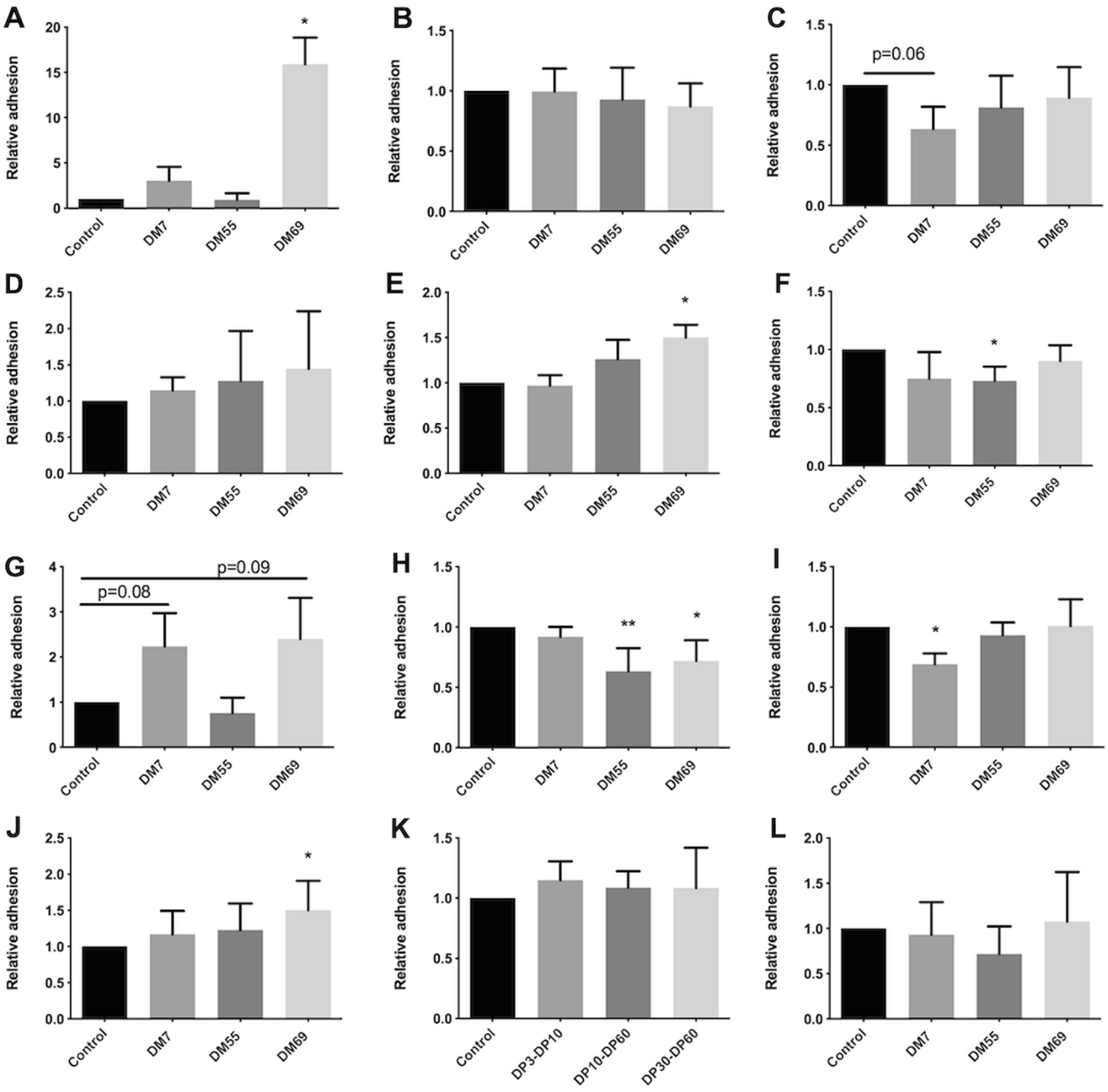

Fig. 3. Decoy effects of pectins on the relative adhesion of pathogens harvested from log and stationary growth phase to gut epithelial Caco-2 cells. Caco-2 cells were cultured for 21 d until confluency. Pathogens were harvested from log or stationary growth phase. The pectins of DM7, DM55, and DM69 were pre-incubated with the pathogens from log phase, *i.e. E. coli* ET8 (A), *E. coli* LMG5862 (B), *E. coli* O119 (C), *E. coli* WA321 (D), *S.* LMG07233 (E), and *K. pneumoniae* LMG20218 (F) or in stationary phase *i.e. E. coli* ET8 (G), *E. coli* LMG5862 (H), *E. coli* O119 (I), *E. coli* WA321 (J), *S.* LMG07233 (K), and *K. pneumoniae* LMG20218 (L) for 2 h. After pre-incubated the individual pathogen with either DM7, DM55, or DM69, the pathogen was applied to Caco-2 cells for the infection for another 2 h. After infection, the total colony forming units (CFUs) of pathogens adhered to Caco-2 cells were determined by a drop-plating method. The group without pectin served as control. All data was expressed as mean ± SD from five experiments. Statistical significance was tested with one-way ANOVA (**$p < 0.01$, *$p < 0.05$).

expression of *E. coli* WA321 was not influenced by the treatment of 3-FL (Figure S3). Fig. 5A shows that with the stimulation of DM69 pectin, 13 genes were up regulated and 57 genes were down regulated in *E. coli* WA321 from the stationary phase. Fig. 5B shows the volcano plot of the expression of all genes of the strain. The extent of the global transcriptome regulation of *E. coli* WA321 in stationary growth phase by DM69 pectin ranged from (log2 fold change) −6.64 to 2.97. Fig. 5C and Table S2 list detailed information about the fold change of the top 10 genes that were significantly ($p \leq 0.05$) up and down regulated, as well as the corresponding GO information. Heatmap analysis (Figure S3) shows the mean value (log2 based) of *E. coli* WA321 in log growth phase with and without 3-FL stimulation, and *E. coli* WA321 in stationary growth phase with and without DM69 pectin stimulation.

3.4.3. DEGs in both pathogens in response to pretreatment with DM69 pectin

Next, venn diagrams were made in order to find stronger evidence for the possible genes that were involved in the increased adhesion of both pathogens with the pretreatment with DM69 pectin. As shown in Fig. 6A and 6B, there were 4 genes significantly up regulated ($p \leq 0.05$) and 44 genes significantly down regulated ($p \leq 0.05$) in both *E. coli* ET8 and *E. coli* WA321 in response to the pretreatment with DM69 pectin. As

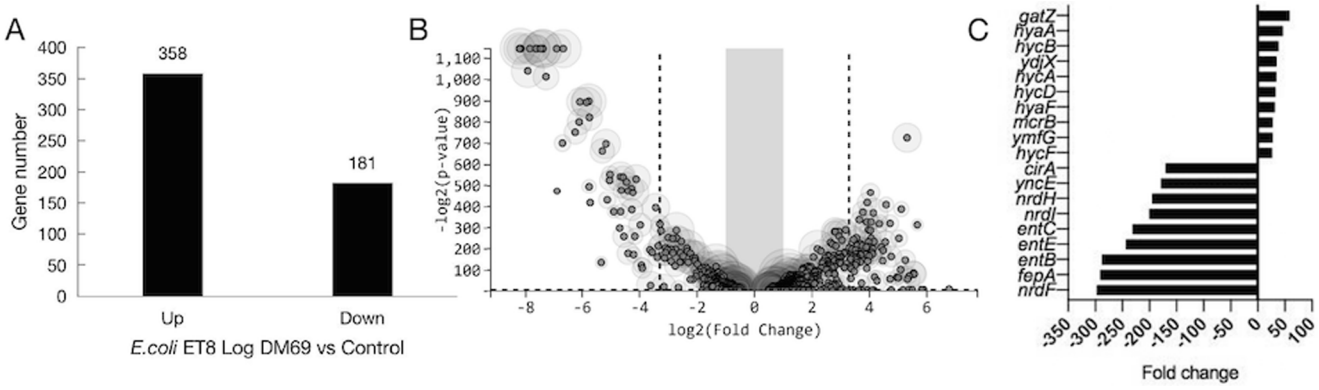

Fig. 4. Analysis of differentially expressed genes (DEGs) of *E. coli* ET8 of log growth phase in response to the stimulation of DM69 pectin. (A) Absolute number of DEGs that were up and down regulated in *E. coli* ET8 of log growth phase in response to the stimulation of DM69 pectin. (B) T-REx generated volcano plot showing the distribution of DEGs that were up and down regulated in *E. coli* ET8 of log growth phase in response to the stimulation of DM69 pectin. Each sphere around a circle stands for a gene measure of the combined expression level of *E. coli* ET8 with and without the stimulation of DM69 pectin. Genes outside the gray area have fold changes ≥ 2 and p values ≤ 0.05, and genes outside the dashed line have fold changes ≥ 8 and p values ≤ 0.01. (C) The top 10 significantly up and down regulated genes in *E. coli* ET8 of log growth phase in response to the stimulation of DM69 pectin.

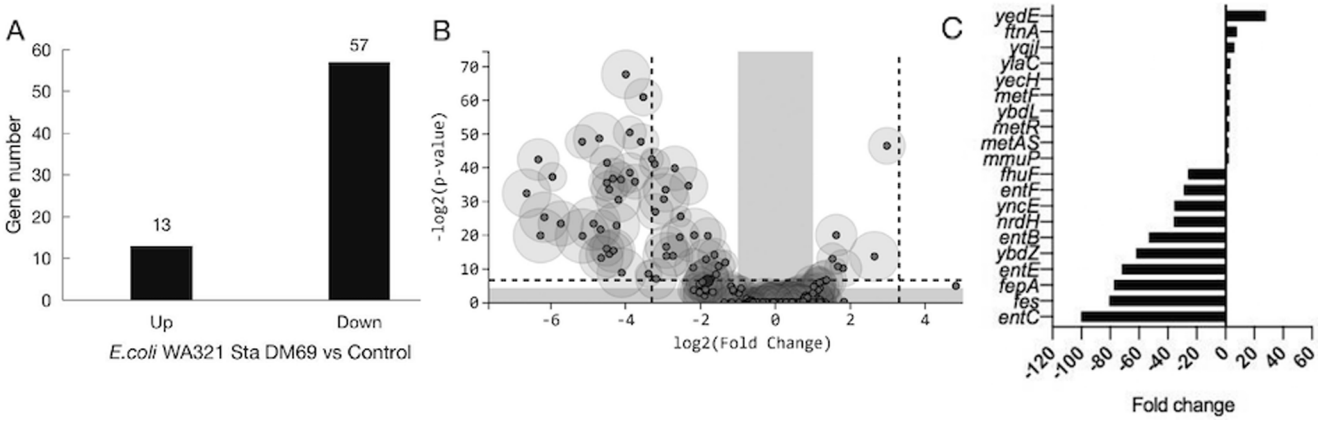

Fig. 5. Analysis of differentially expressed genes (DEGs) of *E. coli* WA321 of stationary growth phase in response to the stimulation of DM69 pectin. (A) Absolute number of DEGs that were up and down regulated in *E. coli* WA321 of stationary growth phase in response to the stimulation of DM69 pectin. (B) T-REx generated volcano plot showing the distribution of DEGs that were up and down regulated in *E. coli* WA321 of stationary growth phase in response to DM69 pectin. Each sphere around a circle stands for a gene measure of the combined expression level of *E. coli* WA321 with and without the stimulation of DM69 pectin. Genes outside the gray area have fold changes ≥ 2 and p values ≤ 0.05, and genes outside the dashed line have fold changes ≥ 8 and p values ≤ 0.01. (C) The top 10 significantly up and down regulated genes in *E. coli* WA321 of stationary growth phase in response to the stimulation of DM69 pectin.

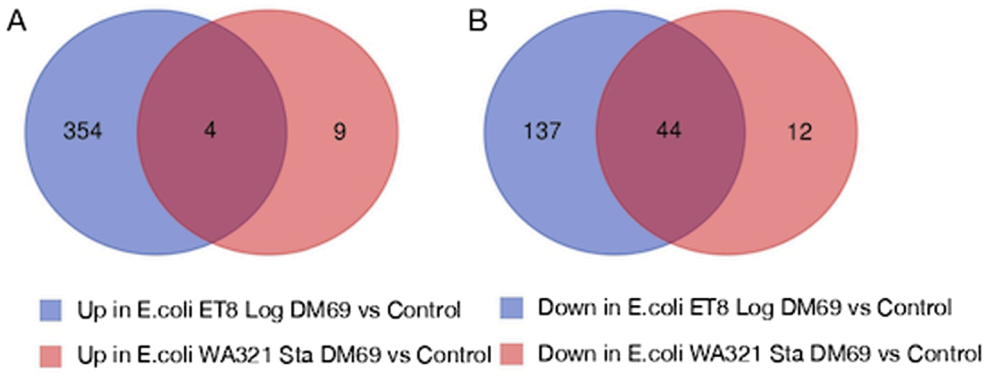

Fig. 6. Venn diagram showing the number of overlapped DEGs that were significantly ($p \leq 0.05$) up (A) and down (B) regulated in *E. coli* ET8 of log phase and *E. coli* WA321 of stationary phase in response to the stimulation of DM69 pectin.

listed in Table 1, the 4 up regulated genes include *yedE*, *yohJ*, *yecH*, and *yqjI*. Among them, *yedE* encodes a membrane protein YedE containing 10 transmembrane regions (Lin et al., 2015), which was 16.4 fold increased in *E. coli* ET8, and 28.1 fold increased in *E. coli* WA321; *yohJ* encodes a putative membrane protein (Flentie et al., 2012) which was 11.7 fold increase in *E. coli* ET8, and 2.0 fold increase in *E. coli* WA321;

Table 1
Significantly up and down regulated genes in both *E. coli* ET8 of log phase and *E. coli* WA321 of stationary phase in response to the stimulation of DM69 pectin.

	Gene	Fold change in *E. coli* ET8	Fold change in *E. coli* WA321	Annotation
Up regulated	*yedE*	16.4	28.1	Predicted Inner Membrane Protein
	yohJ	11.7	2.0	Conserved Inner Membrane Protein
	yecH	7.6	3.2	Hypothetical Protein
	yqjI	7.3	6.2	Predicted Transcriptional Regulator
Down regulated	*nrdF*	−297.2	−25.5	Ribonucleoside-Diphosphate Reductase 2 Subunit Beta
	fepA	−290.7	−77.3	Iron-Enterobactin Outer Membrane Transporter
	entB	−287.6	−53.1	Isochorismatase
	entE	−243.3	−72	Enterobactin Synthase Component E
	entC	−231.3	−100.1	Isochorismate Synthase 1
	nrdI	−200.2	–22.7	Protein That Stimulates Ribonucleotide Reduction
	nrdH	−194.9	−35.8	Glutaredoxin-Like Protein
	yncE	−178.7	−35.6	Conserved Hypothetical Protein
	cirA	−170.0	−17.2	Ferric Iron-Catecholate Outer Membrane Transporter
	nrdE	−169.3	−18.9	Ribonucleoside-Diphosphate Reductase 2 Subunit Alpha
	fes	−156.9	−80.6	Enterobactin/Ferric Enterobactin Esterase
	entD	−121.6	−25.2	Phosphopantetheinyltransferase Component Of Enterobactin Synthase Multienzyme Complex
	ybdZ	−120.1	−62.0	Conserved Hypothetical Protein
	entF	−103.2	−29.0	Enterobactin Synthase Multienzyme Complex Component Atp-Dependent
	fecI	−75.9	−20.2	Probable RNA Polymerase Sigma Factor Feci
	entA	−68.8	−20.0	2,3-Dihydro-2,3-Dihydroxybenzoate Dehydrogenase
	fecR	−67.6	−18.3	Transmembrane Signal Transducer For Ferric Citrate Transport
	fhuF	−54.6	−26.0	Ferric Iron Reductase Involved In Ferric Hydroximate Transport
	fepC	−54.2	–22.6	Iron-Enterobactin Transporter Subunit
	fiu	−53.8	−9.1	Predicted Iron Outer Membrane Transporter
	yddA	−40.4	−10.5	Inner Membrane ABC Transporter ATP-Binding Protein Ydda
	fhuE	−36.1	−21.6	Ferric-Rhodotorulic Acid Outer Membrane Transporter
	fepB	–32.9	−14.8	Iron-Enterobactin Transporter Subunit
	fepG	–32.6	−13.5	Iron-Enterobactin Transporter Subunit
	bfd	−25.9	−9.3	Bacterioferritin-Associated Ferredoxin
	fepD	−25.3	−14.8	Iron-Enterobactin Transporter Subunit
	gpmA	−25.3	−3.5	Phosphoglyceromutase 1
	exbD	−19.5	−7.7	Membrane Spanning Protein In Tonb-Exbb-Exbd Complex
Down regulated	*exbB*	−18.9	−7.9	Membrane Spanning Protein In Tonb-Exbb-Exbd Complex
	sufC	−18.0	−2.3	Component Of Sufbcd Complex Atp-Binding Component Of Abc Superfamily
	fhuA	−17.4	−16.0	Ferrichrome Outer Membrane Transporter
	fecA	−8.5	−7.5	Ferric Citrate Outer Membrane Transporter
	ygaM	−8.5	−3.1	Hypothetical Protein
	ydiE	−7.5	−5.8	Conserved Hypothetical Protein
	fecB	−7.5	−3.9	Iron-Dicitrate Transporter Subunit
	bglJ	−7.2	−17.4	Dna-Binding Transcriptional Regulator
	fecC	−6.8	−4.1	Iron-Dicitrate Transporter Subunit
	yojI	−6.7	−3.6	ABC Transporter ATP-Binding/Permease Protein Yoji
	bfr	−6.1	−2.9	Bacterioferritin Iron Storage And Detoxification Protein
	shiA	−5.0	−3.6	Shikimate Transporter
	feoB	−4.4	−4.5	Fused Ferrous Iron Transporter Protein B
	phoH	−2.9	−3.0	Conserved Hypothetical Protein With Nucleoside Triphosphate Hydrolase Domain
	feoA	−2.6	−3.3	Ferrous Iron Transporter Protein A
	gspO	−2.4	−2.5	Bifunctional Prepilin Leader Peptidase And Methylase

yecH encodes a metal binding hyper-reactive cysteine in YecH protein (Wang et al., 2018), which was 7.6 fold increase in *E. coli* ET8, and 3.2 fold increase in *E. coli* WA321; and *yqjI* encodes a metalloregulatory protein YqjI, responsible for maintaining the biological functions of most proteins for life (Blahut et al., 2018), which was 7.3 fold increased in *E. coli* ET8, and 6.2 fold increased in *E. coli* WA321. Table 1 also lists the 44 genes that were significantly down regulated in both *E. coli* ET8 and *E. coli* WA321 in response to the stimulation of DM69. The top 10 genes were *nrdF, fepA, entB, entE, entC, nrdI, nrdH, yncE, cirA,* and *nrdE.* Among these genes, *nrdE, nrdF, nrdH,* and *nrdI* of the *nrdHIEF* operon are associated with virulence regulation (Roca, Torrents, Sahlin, Gibert, & Sjöberg, 2008), *fepA* and *cirA* are enterobactin receptors (Nedialkova et al., 2014), *entB, entE* and *entC* participate in enterobactin biosynthesis (Butterton, Choi, Watnick, Carroll, & Calderwood, 2000), and *yncE* is associated with high immunoreactive antigen (Roca et al., 2008).

4. Discussion

The hMOs 2′-FL and 3-FL impacted pathogens adhesion differently. 2′-FL did not influence the adhesion of the pathogens, while 3-FL increased the adhesion of *E. coli* WA321 to intestinal epithelial Caco-2 cells. The latter increase was not due to changes in gene regulation, as shown by our transcriptome analysis. The difference between 2′-FL and 3-FL is the linkage of L-fucose, connecting to lactose as a core structure that they both have. That the effects of 3-FL were independent of pathogen metabolism may suggest a possible effect on Caco-2 cells. This is corroborated by a recent observation that 3-FL increases expression of the bacterial adhesion molecule glycosaminoglycans on Caco-2 cells. This was a unique feature of 3-FL and was not observed with L-fucose containing 2′-FL (Kong et al., 2019). Notably, our observation that 2′-FL did not influence pathogen adhesion via a decoy effect should not be interpreted as a suggestion that 2′-FL cannot contribute to lowering of infections. 2′-FL may inhibit pathogen adhesion through other effects such as by impacting the intestinal mucosal layer. It has been shown in mice that 2′-FL inhibited the adhesion of *E. coli* O157 to the intestinal epithelial cells through enhancing *MUC2* expression (Wang et al., 2020). Also, some pathogen strains may be more susceptible for 2′-FL than others as 2′-FL has been reported to have an effect on *Campylobacter*

jejuni pathogenesis and to induce anti-adhesion effects (Yu, Nanthakumar, & Newburg, 2016).

The growth phase dependent effects on pathogens adhesion were most pronounced with inulins. All three tested inulins, *i.e.* DP3-DP10, DP10-DP60, and DP30-DP60, inhibited adhesion of pathogens in log growth phase to Caco-2 cells, but these effects were not observed when the bacteria were in stationary growth phase. In log phase, bacteria grow very fast, which is linked to a high active metabolism. When they enter the stationary phase, the cells face more and more competition for nutrients for survival (Jaishankar & Srivastava, 2017). It is known that bacteria in stationary phase form a much thicker peptidoglycan layer linked to the cell membrane, not only for storing energy, but also to protect essential functions such as the ability to infect eukaryotic cells (Jaishankar & Srivastava, 2017). This thicker peptidoglycan layer may interfere with the ability of oligosaccharide to block pathogen adhesion to Caco-2 cells in stationary phase than in the log phase. Of the six strains tested in log phase, three (*E. coli* LMG5862, *E. coli* WA321, and the lung pathogen *K. pneumoniae* LMG20218) were inhibited by long chain inulin DP30-DP60. DP10-DP60 inulin inhibited *E. coli* O119 and *K. pneumoniae* LMG20218, while short chain inulin DP3-DP10 inhibited only adhesion of *E. coli* O119. The data suggest a chain length-dependent effect of inulins in inhibiting pathogen adhesion to Caco-2 cells, with long chain inulin exhibiting the strongest effect. This is of significant importance for the application of inulin in infant formula, which should preferably contain long chain inulin for anti-pathogenic effects.

Inhibitory effects of pectins on pathogen adhesion to Caco-2 cells were mainly observed when the pathogens were in the stationary phase of growth. For example, DM7 pectin inhibited the adhesion of *E. coli* O119, while DM55 and DM69 pectin repressed the adhesion to Caco-2 cells of *E. coli* LMG5862 in stationary phase. These potent effects of pectins may be explained by their complex structures consisting of a backbone of galacturonic acid and rhamnose, with arabinose and galactose linked branches (Kong, Faas, De Vos, & Akkerman, 2020). These building blocks may provide more blocking points for pathogens (Rhoades et al., 2008). The inhibitory effects of DM7 and DM55 were also observed with *E. coli* O119 and the lung pathogen *K. pneumoniae* LMG20218 in log phase. On the contrary, pectin in a high DM form was also the strongest enhancer of adhesion of certain pathogens on gut epithelial Caco-2 cells, as evidenced by the increased adhesion caused by DM69 pectin exposed *E. coli* ET8 and *S. enterica* subsp *enterica* LMG07233 of log phase and *E. coli* WA321 of stationary phase. The difference in pathogen adhesion to the intestinal epithelial cells between low DM7 pectin and high DM69 pectin may be induced by their different electrical charge. As the low DM pectins have lower numbers of esterified galacturonic acids regions, it is more negatively charged compared to high DM pectin and binds stronger to the positively charged molecules of the intestinal epithelial cells. For example, low DM pectin has been demonstrated to bind stronger to the ligand binding side of Toll-like receptor 2 protein at the side where normally fusion with TLR1 occurs. This ligand binding side contains the positively charged R-arginine and K-lysine amino acids to which low-DM was shown to bind (Sahasrabudhe et al., 2018).

The increasing effects of specific NDCs and hMOs on pathogen adhesion were expected but specific for some NDC structures. Similar observations were reported for several types of hMOs in infection studies with human rotavirus. The hMOs 2′-FL, 3′-SL, and 6-SL reduced the adhesion of the human rotavirus G1P[8] or G2P[4] strains to African green monkey kidney epithelial cells (MA104 cells), while LNT, LNnT or pooled HMOs increased G10P[11] rotavirus adhesion to the cells (Laucirica, Triantis, Schoemaker, Estes, & Ramani, 2017; Ramani et al., 2018). It is widely recognized that both pathogens and commensals can use the intestinal epithelial glycocalyx as the first point of adhesion (Bode & Jantscher-Krenn, 2012). *In vivo,* NDCs are used to increase the adhesion of commensal bacteria such as *Lactobacillus* to compete for binding sites with pathogens, and in this way, inhibit infection (Kong et al., 2020). Our results suggest that certain NDCs, *eg.* DM69 pectin, may in addition to enhancing commensals (Bianchi et al., 2018) also support adhesion of certain pathogens. This implies a risk for application of these types of NDCs in subjects with a low commensal and high pathogen load (Axelrod & Saps, 2018) such as when suffering from irritable bowel syndrome (IBS) (Ihekweazu & Versalovic, 2018). During this period, fermentable NDCs may worsen for that reason IBS symptoms. However, in the field of vaccination, the increased adhesion of pathogens to the epithelial cells with exposure to hMOs has been suggested to be a positive outcome as vaccination efficacy may be enhanced without causing infection (Xiao et al., 2018). To gain insight in how DM69 pectin might help increase the adhesion of certain pathogens, RNA-seq was applied to study gene expression changes in the pathogens. In *E. coli* ET8 of log phase, 358 genes were up regulated and 181 genes were down regulated upon pretreatment of the cells with DM69. Eight of the top10 significantly up regulated genes are known to be involved in adhesion of bacteria to eukaryotic cells. The other two genes, *i.e. ydiX* and *ymfG* have unknown functions. The up-regulated genes *hyaA* and *hyaF* are part of the *hya* operon, and are responsible for [NiFe]-hydrogenase 1 transcription, which supports energy metabolism and can also be involved in enhanced capacity to adhere as *E. coli* strains need much energy supply to use their flagella to spread on epithelium (Berne et al., 2018). DM69 pectin may also strengthen the structure of the flagella of *E. coli* ET8 in log phase as evidenced by the up regulation of 4 genes of the *hyc* operon, *i.e. hycA, hycB, hycD,* and *hycF*. The *hyc* operon dictates activity of the hydrogenase 3 synthesis (Sauter, Böhm, & Böck, 1992) and electron carriers, which is important for the pili assembly (Sanchez, Chang, Wu, Tran, & Ton-That, 2017). Another important reason for more adhesion to Caco-2 cells may be attributed to the up regulation of *gatZ*. This *gatZ* encodes for the D-tagatose-1,6-bisphosphate aldolase subunit and is associated with the catabolism of N-acetylglucosamine (GalNAc) (Kohlmeier, White, Fowler, Finan, & Oresnik, 2019), which is an important component of the glycocalyx of the intestinal epithelial cells and an anchoring point for pathogens (Patsos & Corfield, 2009).

The effect of DM69 pectin was different in *E. coli* WA321, which also demonstrated increased adhesion on Caco-2 cells when harvested from the stationary phase. This seems to be mainly induced by regulating genes involved in the assembly of the outer membrane proteins and biofilm formation. Of the top 10 significantly up regulated genes, the most up regulated gene was *yedE,* which encodes the membrane protein YedE containing 10 transmembrane regions (Lin et al., 2015). The gene function of *yedE* in *Slackia heliotrinireducens* is associated with activation of glycosyltransferase as reported previously (Henikoff, Haughn, Calvo, & Wallace, 1988). This up regulation may suggest that DM69 pectin improves uptake and utilization in *E. coli* WA321 of polysaccharides through enhancing *yedE. yqjI* encodes a metalloregulatory protein YqjI, which is essential for maintaining the biological functions of most proteins (Blahut et al., 2018). *metF, metH, metR, ybdL,* and *mmuP* are involved in the synthesis of methionine, which is an essential amino acid for protein synthesis (Basavanna et al., 2013). Methionine is also a constitute of S-adenosylmethionine which provides methyl group that is required for phospholipids and nucleic acids biosynthesis (Fontecave, Atta, & Mulliez, 2004). In this way, DM69 pectin may improve the acquisition of essential nutrients for *E. coli* WA321, increase bacterial replication and survival (Basavanna et al., 2013), and therefore might be responsible for the increased adhesion. There is also another up regulated gene, *i.e. yecH* that is associated with the amino acid cysteine metabolism (Wang et al., 2018). Methionine and cysteine are two important amino acids in biofilm formation (Nakamura et al., 2016), and therefore likely to be partly responsible for the enhanced adhesion. In particular, the up regulated gene *metF* determines beta-galactosidase level (Stauffer & Stauffer, 1988), which is involved in removal of galactosyl residues from pectin with galactose as reducing end (Kondo et al., 2020). This may imply DM69 pectin increased the ability of *E. coli* WA321 in degrading the galactose branches of pectin as a nutrition supply.

Interestingly our transcriptomics analyses also demonstrated that bacterial virulence might be attenuated despite the DM69 pectin inducing enhanced adhesion of *E. coli* ET8. This is supported by the dramatic decrease (−290 to −55 fold) of the top 10 down regulated genes in *E. coli* ET8. These genes have been reported to be key genes in virulence regulation (*nrdF, nrdH, nrdI,* and *nrdE*), enterobactin receptors (*fepA* and *cirA,*), enterobactin biosynthesis (entB, entE, and entC), or associated with high immunoreactive antigen (*yncE*). Similar results were also obtained in *E. coli* WA321 from the stationary phase when exposed to DM69 pectin. In this case, the top 10 significantly down regulated genes (ranging from −100 to −26 fold) were also involved in bacterial virulence regulation (*nrdH*), and enterobactin receptors, biosynthesis, and processing (*ybdZ, fepA, entF*, *entB*, *entE*, *entC, fes*). Only four genes were up regulated in both *E. coli* ET8 and *E. coli* WA321 incubated with DM69 pectin. These were *yedE, yohJ, yecH,* and *yqjI*. *yedE, yecH,* and *yqjI* are either involved in stabilizing protein functions for life and biofilm formation, and *yohJ* for cell membrane proteins (Flentie, Kocher, Gammon, Novack, & McKinney, 2012). Although only a few studies report the involvement of these genes in bacterial adhesion to the host, protein complexes of *E. coli* strains are critical for the initial adhesion to intestinal epithelial cells (Nadler et al., 2018). These four genes were all up regulated by DM69 pectin in both *E. coli* strains, illustrating that these genes might be responsible for the enhanced bacterial adhesion. Forty-four genes were significantly down regulated in both strains, of which several are associated with either bacterial virulence regulation (*nrdE, nrdF, nrdH,* and *nrdI* of the *nrdHIEF* operon), enterobactin receptors (*fepA* and *cirA*), enterobactin biosynthesis (*entB, entE* and *entC*), or associated with high immunoreactive antigen (*yncE*). Enterobactin biosynthesis and transport genes occupy large sections in a gene cluster (Butterton et al., 2000) in *E. coli* strains. In particular, *cirA* synthesized membrane protein CirA in *E. coli*, is the receptor for colicin Ib (ColIb) produced by *S. serovar Typhimurium* (*S. Tm*) in the inflamed gut (Nedialkova et al., 2014). DM69 pectin may reduce ColIb mediated competitive killing between *E. coli* and *S. Tm* through down regulation of *cirA*. Also, the virulence of *E. coli* ET8 and *E. coli* WA321 might be attenuated by DM69 pectin through downregulation of *cirA*. This argument is supported by the observation that inactivation of *cirA* in *S.* Enteritidis C50336 attenuated virulence of the strain in a mice study (Zhang et al. 2020).

5. Conclusion

In conclusion, here NDCs including inulins and pectins were shown to inhibit the adhesion of gut pathogens to intestinal epithelial Caco-2 cells by serving as decoy receptors as hypothesized. The inhibition effects are chemical structure dependent. Especially inulins and low DM pectin have such an effect, while 3-FL and high DM pectin DM69 increased bacterial adhesion. 3-FL does not seem to change metabolism in the pathogen *E. coli* WA321, but rather, as reported before, enhance anchoring points for pathogens on gut epithelial cells (Kong et al., 2019). DM69 pectin strongly changes behavior of the pathogens *E. coli* ET8 and *E. coli* WA321, and increases pathogens adhesion through up regulation of flagella and other cell membrane proteins associated genes. However, the increased adhesion should not be interpreted as increased infection as bacterial virulence associated genes of the pathogens were reduced. Our data contributes to a better understanding of the decoy effects of certain dietary fibers on pathogens, and provide new means to design “tailored” infant formula, especially for preterm infants at risk for pathogen infections.

CRediT authorship contribution statement

Chunli Kong: Conceptualization, Methodology, Formal analysis, Investigation, Writing – original draft. **Anne de Jong:** Software, Formal analysis, Data curation. **Bart J. de Haan:** Methodology, Investigation. **Jan Kok:** Conceptualization, Writing – review & editing. **Paul de Vos:** Conceptualization, Supervision, Writing – review & editing, Project administration.

Declaration of Competing Interest

The authors declare that they have no known competing financial interests or personal relationships that could have appeared to influence the work reported in this paper.

Acknowledgements

The study was financially supported by the China Scholarship Council (CSC). This research was performed within the framework of Sino-Dutch Doctoral Program on Sustainable Dairy coordinated by the Carbohydrate Competence Center (CCC, http://www.cccresearch.nl).

Appendix A. Supplementary data

Supplementary data to this article can be found online at https://doi.org/10.1016/j.foodres.2021.110867.

References

Asakuma, S., Hatakeyama, E., Urashima, T., Yoshida, E., Katayama, T., Yamamoto, K., … Kitaoka, M. (2011). Physiology of consumption of human milk oligosaccharides by infant gut-associated bifidobacteria. *Journal of Biological Chemistry, 286*(40), 34583–34592.

Axelrod, C. H., & Saps, M. (2018). The role of fiber in the treatment of functional gastrointestinal disorders in children. *Nutrients, 10*(11), 1650–1666.

Basavanna, S., Chimalapati, S., Maqbool, A., Rubbo, B., Yuste, J., Wilson, R. J., … Brown, J. S. (2013). The effects of methionine acquisition and synthesis on *Streptococcus pneumoniae* growth and virulence. *PLoS ONE, 8*(1), Article e49638.

Berne, C., Ellison, C. K., Ducret, A., & Brun, Y. V. (2018). Bacterial adhesion at the single-cell level. *Nature Reviews Microbiology, 16*(10), 616–627.

Bianchi, F., Larsen, N., de Mello Tieghi, T., Adorno, M. A. T., Kot, W., Saad, S. M. I., … Sivieri, K. (2018). Modulation of gut microbiota from obese individuals by in vitro fermentation of citrus pectin in combination with *Bifidobacterium longum* BB-46. *Applied Microbiology and Biotechnology, 102*(20), 8827–8840.

Blahut, M., Dzul, S., Wang, S., Kandegedara, A., Grossoehme, N. E., Stemmler, T., & Outten, F. W. (2018). Conserved cysteine residues are necessary for nickel-induced allosteric regulation of the metalloregulatory protein YqjI (NfeR) in *E. coli*. *Journal of Inorganic Biochemistry, 184*, 123–133.

Bode, L., & Jantscher-Krenn, E. (2012). Structure-function relationships of human milk oligosaccharides. *Advances in Nutrition (Bethesda, Md.), 3*(3), 383S–391S.

Butterton, J. R., Choi, M. H., Watnick, P. I., Carroll, P. A., & Calderwood, S. B. (2000). *Vibrio cholerae* VibF is required for vibriobactin synthesis and is a member of the family of nonribosomal peptide synthetases. *Journal of Bacteriology, 182*(6), 1731–1738.

Carvalho, G. G., Calarga, A. P., Teodoro, J. R., Queiroz, M. M., Astudillo-Trujillo, C. A., Levy, C. E., … Kabuki, D. Y. (2020). Isolation, comparison of identification methods and antibiotic resistance of *Cronobacter* spp. in infant foods. *Food Research International, 137*, Article 109643.

Chen, P., Reiter, T., Huang, B., Kong, N., & Weimer, B. C. (2017). Prebiotic oligosaccharides potentiate host protective responses against *L. monocytogenes* infection. *Pathogens, 6*(4), 68–93.

Cheng, L., Akkerman, R., Kong, C., Walvoort, M. T. C., & de Vos, P. (2020). More than sugar in the milk: Human milk oligosaccharides as essential bioactive molecules in breast milk and current insight in beneficial effects. *Critical Reviews in Food Science and Nutrition, 61*(7), 1184–1200.

Coppa, G. V., Zampini, L., Galeazzi, T., Facinelli, B., Ferrante, L., Capretti, R., & Orazio, G. (2006). Human milk oligosaccharides inhibit the adhesion to Caco-2 cells of diarrheal pathogens: *Escherichia coli, Vibrio cholerae,* and *Salmonella fyris*. *Pediatric Research, 59*(3), 377–382.

Daniell, S. J., Delahay, R. M., Shaw, R. K., Hartland, E. L., Pallen, M. J., Booy, F., … Frankel, G. (2001). Coiled-coil domain of enteropathogenic *Escherichia coli* type III secreted protein EspD is involved in EspA filament-mediated cell attachment and hemolysis. *Infection and Immunity, 69*(6), 4055–4064.

de Jong, A., van der Meulen, S., Kuipers, O. P., & Kok, J. (2015). T-REx: Transcriptome analysis webserver for RNA-seq Expression data. *BMC Genomics, 16*(1), 663–669.

Flentie, K., Kocher, B., Gammon, S. T., Novack, D. V., McKinney, J. S., & Piwnica-Worms, D. (2012). A bioluminescent transposon reporter-trap identifies tumor-specific microenvironment-induced promoters in *Salmonella* for conditional bacterial-based tumor therapy. *Cancer Discovery, 2*(7), 624–637.

Fontecave, M., Atta, M., & Mulliez, E. (2004). S-adenosylmethionine: Nothing goes to waste. *Trends in Biochemical Sciences, 29*(5), 243–249.

Henikoff, S., Haughn, G. W., Calvo, J. M., & Wallace, J. C. (1988). A large family of bacterial activator proteins. *Proceedings of the National Academy of Sciences of the United States of America, 85*(18), 6602–6606.

Herigstad, B., Hamilton, M., & Heersink, J. (2001). How to optimize the drop plate method for enumerating bacteria. *Journal of Microbiological Methods, 44*(2), 121–129.

Heymann, J., Raub, A., & Earle, A. (2013). Breastfeeding policy: A globally comparative analysis. *Bulletin of the World Health Organization, 91*(6), 398–406.

Holscher, H. D., Bode, L., & Tappenden, K. A. (2017). Human milk oligosaccharides influence intestinal epithelial cell maturation in vitro. *Journal of Pediatric Gastroenterology and Nutrition, 64*(2), 296–301.

Ihekweazu, F. D., & Versalovic, J. (2018). Development of the Pediatric Gut Microbiome: Impact on Health and Disease. *American Journal of the Medical Sciences, 356*(5), 413–423.

Jaishankar, J., & Srivastava, P. (2017). Molecular basis of stationary phase survival and applications. *Frontiers in Microbiology, 8*, 2000–2012.

Kiewiet, M. B. G., Dekkers, R., van Gool, M. P., Ulfman, L. H., Groeneveld, A., Faas, M. M., & de Vos, P. (2018). Identification of a TLR2 inhibiting wheat hydrolysate. *Molecular Nutrition and Food Research, 62*(23), Article e1800716.

Kohlmeier, M. L. G., White, C. E., Fowler, J. E., Finan, T. M., & Oresnik, I. J. (2019). Galactitol catabolism in *Sinorhizobium meliloti* is dependent on a chromosomally encoded sorbitol dehydrogenase and a pSymB-encoded operon necessary for tagatose catabolism. *Molecular Genetics and Genomics, 294*(3), 739–755.

Kondo, T., Nishimura, Y., Matsuyama, K., Ishimaru, M., Nakazawa, M., Ueda, M., & Sakamoto, T. (2020). Characterization of three GH35 β-galactosidases, enzymes able to shave galactosyl residues linked to rhamnogalacturonan in pectin, from *Penicillium chrysogenum* 31B. *Applied Microbiology and Biotechnology, 104*(3), 1135–1148.

Kong, C., Elderman, M., Cheng, L., de Haan, B. J., Nauta, A., & de Vos, P. (2019). Modulation of intestinal epithelial glycocalyx development by human milk oligosaccharides and non-digestible carbohydrates. *Molecular Nutrition and Food Research, 63*(17), Article e1900303.

Kong, C., Faas, M. M., De Vos, P., & Akkerman, R. (2020). Impact of dietary fibers in infant formulas on gut microbiota and the intestinal immune barrier. *Food and Function, 11*(11), 9445–9467.

Laucirica, D. R., Triantis, V., Schoemaker, R., Estes, M. K., & Ramani, S. (2017). Milk oligosaccharides inhibit human rotavirus infectivity in MA104 cells. *The Journal of Nutrition, 147*(9), 1709–1714.

Lin, J., Peng, T., Jiang, L., Ni, J. Z., Liu, Q., Chen, L., & Zhang, Y. (2015). Comparative genomics reveals new candidate genes involved in selenium metabolism in prokaryotes. *Genome Biology and Evolution, 7*(3), 664–676.

Nadler, H., Shaulov, L., Blitsman, Y., Mordechai, M., Jopp, J., Sal-Man, N., & Berkovich, R. (2018). Deciphering the mechanical properties of type III secretion system EspA protein by single molecule force spectroscopy. *Langmuir., 34*(21), 6261–6270.

Nakamura, Y., Yamamoto, N., Kino, Y., Yamamoto, N., Kamei, S., Mori, H., … Nakashima, N. (2016). Establishment of a multi-species biofilm model and metatranscriptomic analysis of biofilm and planktonic cell communities. *Applied Microbiology and Biotechnology, 100*(16), 7263–7279.

Nedialkova, L. P., Denzler, R., Koeppel, M. B., Diehl, M., Ring, D., Wille, T., … Stecher, B. (2014). Inflammation fuels colicin Ib-dependent competition of *Salmonella* serovar typhimurium and *E. coli* in *Enterobacterial* blooms. *PLoS Pathogens, 10*(1), Article e1003844.

Patsos, G., & Corfield, A. (2009). Management of the human mucosal defensive barrier: Evidence for glycan legislation. *Biological Chemistry, 390*(7), 581–590.

Peterson, J. W. (1996). Medical Microbiology. In B. S. (Ed.), *Medical Microbiology* (4th ed.). Galveston.

Ramani, S., Stewart, C. J., Laucirica, D. R., Ajami, N. J., Robertson, B., Autran, C. A., … Estes, M. K. (2018). Human milk oligosaccharides, milk microbiome and infant gut microbiome modulate neonatal rotavirus infection. *Nature Communication, 9*(1), 5010.

Rhoades, J., Manderson, K., Wells, A., Hotchkiss, A. T., Gibson, G. R., Formentin, K., … Rastall, R. A. (2008). Oligosaccharide-mediated inhibition of the adhesion of pathogenic *Escherichia coli* strains to human gut epithelial cells in vitro. *Journal of Food Protection, 71*(11), 2272–2277.

Roca, I., Torrents, E., Sahlin, M., Gibert, I., & Sjöberg, B. M. (2008). NrdI essentiality for class Ib ribonucleotide reduction in *Streptococcus pyogenes*. *Journal of Bacteriology, 190*(14), 4849–4858.

Ruiz-Palacios, G. M., Cervantes, L. E., Ramos, P., Chavez-Munguia, B., & Newburg, D. S. (2003). *Campylobacter jejuni* binds intestinal H(O) antigen (Fucα1, 2Galβ1, 4GlcNAc), and fucosyloligosaccharides of human milk inhibit its binding and infection. *Journal of Biological Chemistry, 278*(16), 14112–14120.

Sahasrabudhe, N. M., Beukema, M., Tian, L., Troost, B., Scholte, J., Bruininx, E., … de Vos, P. (2018). Dietary fiber pectin directly blocks Toll-like receptor 2–1 and prevents doxorubicin-induced ileitis. *Frontiers in Immunology, 9*, 383.

Sanchez, B. C., Chang, C., Wu, C., Tran, B., & Ton-That, H. (2017). Electron transport chain is biochemically linked to pilus assembly required for polymicrobial interactions and biofilm formation in the gram-positive actinobacterium *Actinomyces oris*. *MBio, 8*(3), Article e00399.

Sauter, M., Böhm, R., & Böck, A. (1992). Mutational analysis of the operon (hyc) determining hydrogenase 3 formation in *Escherichia coli*. *Molecular Microbiology, 6*(11), 1523–1532.

Stauffer, G. V., & Stauffer, L. T. (1988). *Salmonella typhimurium* LT2 metF operator mutations. *MGG Molecular & General Genetics, 214*(1), 32–36.

Thöle, C., Brandt, S., Ahmed, N., & Hensel, A. (2015). Acetylated rhamnogalacturonans from immature fruits of *Abelmoschus esculentus* inhibit the adhesion of *Helicobacter pylori* to human gastric cells by interaction with outer membrane proteins. *Molecules, 20*(9), 16770–16787.

Urashima, T., Taufik, E., Fukuda, K., & Asakuma, S. (2013). Recent advances in studies on milk oligosaccharides of cows and other domestic farm animals. *Bioscience Biotechnology and Biochemistry, 77*(3), 455–466.

Walker, S. L., Hill, J. E., Redman, J. A., & Elimelech, M. (2005). Influence of growth phase on adhesion kinetics of *Escherichia coli* D21g. *Applied and Environmental Microbiology, 71*(6), 3093–3099.

Wang, H., Chen, X., Li, C., Liu, Y., Yang, F., & Wang, C. (2018). Sequence-based prediction of cysteine reactivity using machine learning. *Biochemistry, 57*(4), 451–460.

Wang, Y., Zou, Y., Wang, J., Ma, H., Zhang, B., & Wang, S. (2020). The protective effects of 2'-fucosyllactose against *E. coli* O157 infection are mediated by the regulation of gut microbiota and the inhibition of pathogen adhesion. *Nutrients, 12*(5), 1284.

Xiao, L., Leusink-Muis, T., Kettelarij, N., van Ark, I., Blijenberg, B., Hesen, N. A., … Van't Land, B. (2018). Human milk oligosaccharide 2'-fucosyllactose improves innate and adaptive immunity in an influenza-specific murine vaccination model. *Frontiers in Immunology, 9*, 452.

Yu, Z., Nanthakumar, N. N., & Newburg, D. S. (2016). The human milk oligosaccharide 2'-fucosyllactose quenches *Campylobacter jejuni*-induced inflammation in human epithelial cells HEp-2 and HT-29 and in mouse intestinal mucosa. *The Journal of Nutrition, 146*(10), 1980–1990.

Zhang, Z., Du, W., Wang, M., Li, Y., Su, S., Wu, T., … Zhu, G. (2020). Contribution of the colicin receptor CirA to biofilm formation, antibotic resistance, and pathogenicity of *Salmonella* Enteritidis. *Journal of Basic Microbiology, 60*(1), 72–81.